N91-17077

Fixed-Head Star Tracker Magnitude Calibration on the Solar Maximum Mission

D.S. Pitone, B.J. Twambly, A.H. Eudell, and D.A. Roberts
Computer Sciences Corporation (CSC)

ABSTRACT

The sensitivity of the fixed-head star trackers (FHSTs) on the Solar Maximum Mission (SMM) is defined as the accuracy of the electronic response to the magnitude of a star in the sensor field-of-view, which is measured as intensity in volts. To identify stars during attitude determination and control processes, a transformation equation is required to convert from star intensity in volts to units of magnitude and vice versa. To maintain high accuracy standards, this transformation is calibrated frequently. A sensitivity index is defined as the observed intensity in volts divided by the predicted intensity in volts; thus, the sensitivity index is a measure of the accuracy of the calibration. Using the sensitivity index, analysis is presented that compares the strengths and weaknesses of two possible transformation equations. The effect on the transformation equations of variables, such as position in the sensor field-of-view, star color, and star magnitude, is investigated. In addition, results are given that evaluate the aging process of each sensor. The results in this work can be used by future missions as an aid to employing data from star cameras as effectively as possible.

1. INTRODUCTION

From the time of the repair of the Solar Maximum Mission (SMM) in April 1984 to its reentry in December 1989, an enormous amount of attitude sensor data were collected. The fixed-head star trackers (FHSTs) on the SMM during this time primarily collected two types of data. The first, star position in the FHST field-of-view (FOV), provided after transformation by the FHST alignment matrix, observed star position vectors in the body frame for SMM attitude determination. The second, star intensity data, were used for star identification purposes. Star intensity is the FHST measurement of the magnitude of the star. This paper is concerned with this second type of data, primarily what is the most effective way to calibrate the FHSTs' electronic response to stellar magnitude and how may the FHST magnitude data be used to give some insight into how the electro-optical components of the FHSTs aged over the lifetime of the SMM. These data, in turn, may then be used to aid analysis for future missions that employ similar types of star cameras for attitude determination and control.

For the SMM, visual stellar magnitude was used for star identification. This identification was necessary for both attitude determination and attitude control of the spacecraft. For attitude determination, the observed intensity was taken from the raw FHST data, converted to visual magnitude using a calibrated transformation equation, and then used

to help identify the observed star. Using the identity of the observed star, the corresponding representation in Geocentric Inertial (GCI) coordinates from the star catalog are used to form a reference vector. The reference vector and the observed vector are then used along with other pairs of reference and observed vectors in an algorithm to determine the attitude.

Stellar magnitude was used for attitude control to maintain the current attitude of the spacecraft. Using ground based software, stars useful for control at specific attitudes and time periods were selected from the star catalog. The expected positions of these stars in the FHST FOV and their predicted magnitudes were then uplinked to the spacecraft. The catalog magnitude was transformed to intensity in volts, again using the calibrated transformation equation. The FHST then searched for these stars, called guide stars, at the predicted coordinates in the FOV. If a star was observed within a specified angular distance, usually one tenth of a degree (deg), of the predicted location, its intensity was compared with the predicted intensity. If they matched, again within a specified tolerance, it was assumed that the correct guide star had been located. Discrepancies in the position of the guide star in the FHST FOV were then attributed to error in the spacecraft attitude, and the spacecraft would be rotated to null the discrepancy. Thus, the spacecraft attitude was maintained.

The preceding paragraphs show that stellar magnitude is important for accurate spacecraft attitude determination and control. Thus, the equation that related magnitude and intensity was calibrated periodically to maintain an accurate transformation.

This work has two major goals. The first is to evaluate two possible transformation equations for accuracy and ease of application. In addition, the various parameters that effect the optical sensitivity of the FHST will be examined and correlated to sensitivity. The second goal is to establish a method for investigating the aging process of star cameras. It is apparent that as the sensor ages, it will become less sensitive. Methods for examining the rate of aging are presented along with results for the SMM FHSTs.

The paper is organized as follows: Section 2 provides a brief history of the mission, along with the basic configuration of the attitude determination and control system of the spacecraft. Section 3 includes a description of the FHST hardware aboard the SMM and the mathematical models used to reduce the FHST data. Section 4 outlines the analysis performed to calibrate the intensity-to-magnitude transformation equation, including an investigation of two possible transformation equations and the actual calibration results. Section 5 considers how the results of the calibrations may be used to gain insight into the aging process of the electro-optical components of the FHST. This provides information about the duration of reliability these type of star cameras have in space.

2. THE SOLAR MAXIMUM MISSION

Mission History

The SMM was launched in February 1980 from the Eastern Test Range at Kennedy Space Center into an approximately circular low-Earth orbit, with an inclination near 28 deg. The scientific objective of the mission was the study of solar phenomena. The spacecraft attitude system provided three-axis stabilization and supported solar feature

targeting. The spacecraft functioned normally until November 1980, when the standard reaction wheel (SRW) package that provided the controlling torques to the spacecraft began to fail. To preserve the mission, the SMM was put into a spin (approximately 1 deg per second (sec)) about the minor principal axis. During April 1984, the spacecraft was repaired in-orbit as part of a Space Transportation System (STS) mission. The entire attitude control system was replaced, and the spacecraft was returned to the nominal scientific observing mode. The spacecraft functioned normally until August 1987, when one of the two Ball Aerospace CT401 FHSTs sustained a failure in the power supply to the sensor. Since the spacecraft had two FHSTs, this loss had only a minimal effect on the attitude determination and control of the spacecraft. On December 2, 1989, the SMM reentered the Earth's atmosphere. The surviving remnants crashed into the Indian Ocean. Further details on the history of the SMM are available in Ref. 1.

Mission Configuration

The SMM was the first of the multimission modular spacecraft (MMS) series that were modular to facilitate mission repair and adaptation. The SMM basically consisted of two parts: the MMS itself and the experiment module. The components that came with the MMS series were a communications module, a power module, and a modular attitude control system (MACS). The SMM FHSTs were located in the MACS. The experiment module contained all the SMM mission-specific components, including the SMM scientific instruments and the mission-specific attitude sensors. The instruments comprising the scientific payload were designed to study the Sun at several different wavelengths of light, including gamma, X-ray, and ultraviolet.

3. SMM FHST DESCRIPTION

Hardware Description

The SMM FHSTs were National Aeronautics and Space Administration (NASA) Standard Star Trackers (SST), manufactured by Ball Aerospace Systems Division. An SST is an electro-optical instrument that uses an image dissector to search for and track stars[2]. It provides star position and magnitude information about a two-axis coordinate system in an eight-by-eight deg FOV. The accuracy of the two-axis position information is 10 arc-sec (1σ) when fully calibrated and is output as counts. The transformation equation from counts to degrees is calibrated for star temperature and intensity, and the magnetic field.

The SST is protected against bright light by a shutter. When the bright object alert sensor (BOAS) is triggered, the shutter closes, protecting the SST. When the BOAS senses that the bright object is out of the FOV of the SST, the shutter is reopened.

After the shutter is opened, the SST starts out in a search mode. The instrument will search the total FOV by scanning, as shown in Fig. 1. This scan takes approximately 10 sec to search the complete FOV. The search scan continues until a star is sensed. At this point the SST enters the track scan mode. The track scan mode forms a smaller cross-pattern that repeats approximately 100 times per sec. This pattern is also shown in Fig. 1. The track scan mode provides many observations of the same star. A threshold is set that

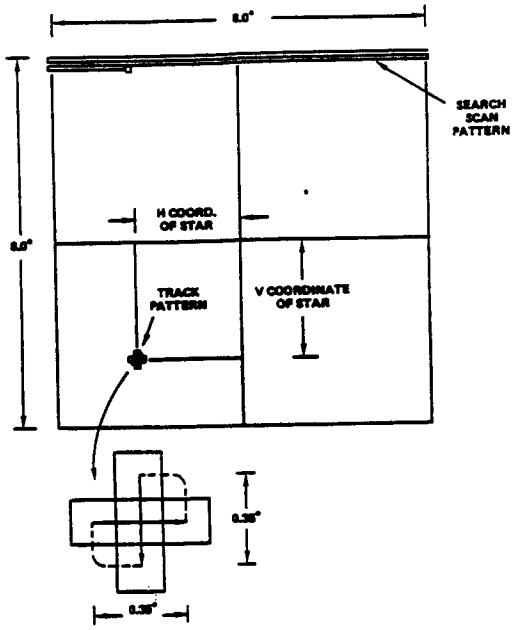

Figure 1. FHST Field-of-View

provides a break-track command that forces the SST back to the search mode. Thus, the SST operates by searching for a star, entering track mode, providing many observations of that star, and then reentering search mode until another star is found. This pattern is repeated until the BOAS is triggered, and the shutter is closed.

When a star is tracked, light from the star enters the lens. The image is focused on the photocathode of the image dissector tube (IDT). The optical image is converted to an electron image at the photocathode, and this image is refocused at the IDT aperture plate. A small aperture passes a portion of the electron image to the electron multiplier. The signal is multiplied and sent to the video processing electronics where it is demodulated. At this point, star intensity and position information are obtained. Further details on the hardware of the SMM FHSTs are available in Ref. 2.

Mathematical Description

Each FHST provided star position about two sensor axes and star magnitude information to the SMM onboard computer (OBC), where it was time tagged and subsequently telemetered to the ground. Each star observation was telemetered as three pieces of data. The first piece was the angle from the first sensor coordinate axis for a specific star at the time tagged by the OBC. The second piece of data was the angle from the second sensor coordinate axis for the same star at the same time. The sensed stellar intensity of the

observation, the third piece of data, had units of voltage.

For use in attitude determination and control algorithms, the raw FHST data are converted to usable quantities. As shown in Fig. 1, the SMM FHSTs had two output axes, horizontal and vertical. The first piece of position data was the angular length of the observed star vector's projection onto the horizontal axis, labeled the H coordinate. The second piece of data was the angular length of the observed star vector's projection onto the vertical axis, labeled the V coordinate. The H and V coordinates were then calibrated for the effects mentioned earlier and transformed to degrees[3]. From the H and V coordinates, a vector representing the direction of the observed star in the FHST sensor coordinate frame was formed. This vector was then transformed to the body frame by the FHST alignment matrix for use in the attitude determination algorithm.

The magnitude data were reduced by simply transforming the intensity in volts to magnitude. There are several general equations to accomplish this. Much of the remainder of this paper is concerned with which of two possible candidates was thought to be best for the SMM, i.e., provided the most usable results.

4. ANALYSIS

Data Collection

Because of the large volume of FHST data collected during the flight of the SMM, data reduction was necessary for presentability. It was assumed that the processes that changed the sensitivity were not instantaneous, and, in practice, it was found that large changes took 6 months to 1 year to occur. In addition, about 3 months of data needed to be collected to provide meaningful results. Thus, the periods of data collection were defined as presented in Table 1. The selection of the exact time periods during the year depended on the availability of data.

Table 1. FHST Data Interval Timespans

FHST 1		**FHST 2**	
October - December	1984	October - December	1984
July - September	1985	July - September	1985
January - March	1986	June - August	1986
July - September	1987	June - August	1987
July - September	1988		
March - May	1989		

The exact nature of the data collected during the timespans was chosen to facilitate the analysis in each of the goals of this work. From the FHST telemetry, each observation was tagged with the observation time, FHST ID, horizontal and vertical coordinates, and observed intensity. From the SKYMAP star catalog[4], the star identification number, predicted magnitude, and star color represented as the difference in blue and visual magnitude were collected for each observation.

Mathematical Definitions

To gauge the accuracy of the transformation from visual magnitude to FHST intensity the ratio of observed, I_o, to predicted intensity, I_p, is used. Thus the sensitivity value, S, is defined to be

$$S \equiv I_o / I_p \quad . \tag{3-1}$$

Observed intensities were provided directly from telemetry as voltages. Predicted intensities were calculated by one of two transformation equations. The more accurate the transformation equation, the closer the sensitivity value would be to 1 for an observation.

To correlate the calculated sensitivity values with position, each FHST FOV was divided into 0.2 × 0.2 deg squares. For each observation, a sensitivity value was calculated and, using the observed H and V coordinates, associated with a 0.2 × 0.2 deg square. All the sensitivity values for a particular timespan and square were then averaged to obtain one sensitivity value for each square.

Evaluation of Two Transformation Equations

Although there are many ways the transformation from magnitude to intensity could be represented, this work will consider two that show considerable promise but for different reasons. The first is a simple conversion from intensity to magnitude based on the logarithmic scale of magnitude. The logarithm of the intensity is multiplied by a calibrated scale factor and added to a calibrated bias. Thus,

$$\mathrm{M} = A * \log_{10}(I_p) + B \quad , \tag{3-2}$$

where M is the visual magnitude from the SKYMAP catalog, and A and B are the calibration coefficients. This equation lacks any term for star color dependence or FOV position. The second equation was recommended for use on SMM before launch[5]. In fact, this analysis is a result of analysis recommended in that report. The equation has the form

$$\mathrm{M} = A_o + A_1 H + A_2 V + A_3 H^2 + A_4 HV + A_5 V^2 - 2.5 \log_{10}(I_p) \quad , \tag{3-3}$$

where H and V are the FHST coordinates and the A_i's are defined as

$$A_i = \alpha_{i0} + \alpha_{i1}(B - V) + \alpha_{i2}(B - V)^2 \quad , \tag{3-4}$$

where $B - V$ represents the star color and the α_{ij}'s are the calibration coefficients.

During the initial FHST data processing, Equation (3-2) was used to reduce the data because it was thought at the time that it would provide adequate results while greatly easing implementation. Thus, this assumption may be tested using the actual data.

To perform the tests, the calibration coefficients for each equation were calculated for each segment of data in Table 1. Since Equation (3-2) was used throughout the mission, its calibration coefficients were available directly from the SMM archives. The coefficients in Equation (3-4) were calculated using a small sample of data before each 3-month data segment. Then the observations in each segment were reduced using the equations, and the results were graphed and assembled in tables.

Fig. 2 through Fig. 5 show typical results for each equation. In the figures, the small boxes are the 0.2 × 0.2 deg data sample squares. If the box is empty, the sensitivity value is between 0.95 and 1.05, i.e., it is within 5 percent of the expected value. If the box is filled, then the sensitivity value is either less than 0.95 or greater than 1.05. Thus, dark areas represent the areas of an FHST where stellar magnitude will be sensed less accurately. Areas of the FOV with no sample boxes were areas with no data during that timespan.

The results in these figures show the superiority of the polynomial transformation. Fig. 2 represents the simple transformation for the July through September 1988 time segment. The large area of poor sensitivity in the -V half of the FOV, especially in the -V,+H quadrant, should be noted. Fig. 3 is the same data fit with the polynomial transformation. The reduction in the number of boxes with poor sensitivity values and the lack of any concentrated area with poor sensitivity should also be noted. Figs. 4 and 5 show a similar improvement in FHST2 between the simple and polynomial transformations.

These improvements are expected because the polynomial transformation fully accounts for all the factors. We now address the question of whether the improvement is worth the effort and computer memory needed to obtain it?

Further analysis of the comparison and an examination of the errors that result from poor FHST sensitivity can resolve this question. The complete comparison results are provided in Tables 2 and 3. The columns entitled Simple and Polynomial provide the important numbers for the comparison study. The column entitled Original contains the data that illustrates FHST aging, which is addressed later. Table 2 presents comparison data for the total FOV of each data segment while Table 3 is confined to the -V,+H quadrant of FHST1. The numbers in the columns represent the percentage of the total number of observed sample boxes that have sensitivity within 10 percent of unity. The data in both tables show that the polynomial transformation yields significantly better results.

The type of error that can occur from a lack of sensitivity is a misidentification of a star. For the SMM, this misidentification mainly affected the attitude control. If a star was misidentified during the attitude determination process, the observation was simply discarded. Since there were usually many observations, discarding one observation did not significantly affect the attitude determination. However, the SMM used guide stars to control the spacecraft. An identification error could take two forms. First, the wrong star could be identified as the guide star. Thus, the spacecraft would correct its attitude by rotating to place the misidentified star in the predicted position in the FHST FOV. This would cause the attitude of the spacecraft to be in error. Adding to this error would be the fact that the OBC would indicate the attitude was correct because it believed it had identified the correct guide star.

The second type of identification error occurred when the guide star could not be located by the search pattern. This happened because the guide star intensity was so poorly predicted; no observed star whose intensity matched the prediction could be found. Thus, the attitude of the spacecraft would not be corrected and an error would accrue.

Because of the high accuracy requirements of the SMM, both of these situations would cause significant errors in the roll attitude of the spacecraft. However, only in several isolated incidents was the roll error higher than the 0.1 deg roll error limit. At these times, the roll attitude was computed by the ground support system, and the spacecraft was

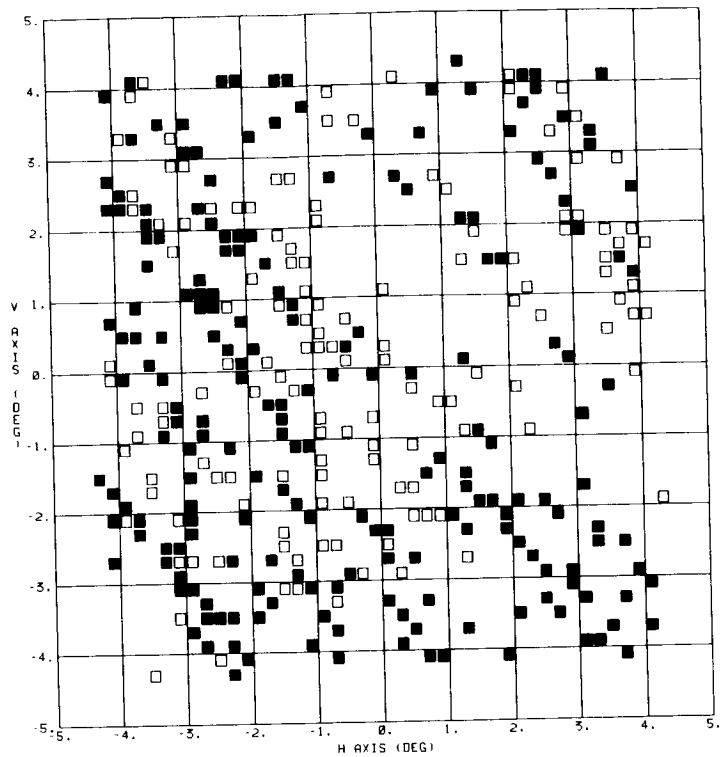

Figure 2. FHST1 Sensitivity Index Plot Using Simple Transformation, 1988 Data

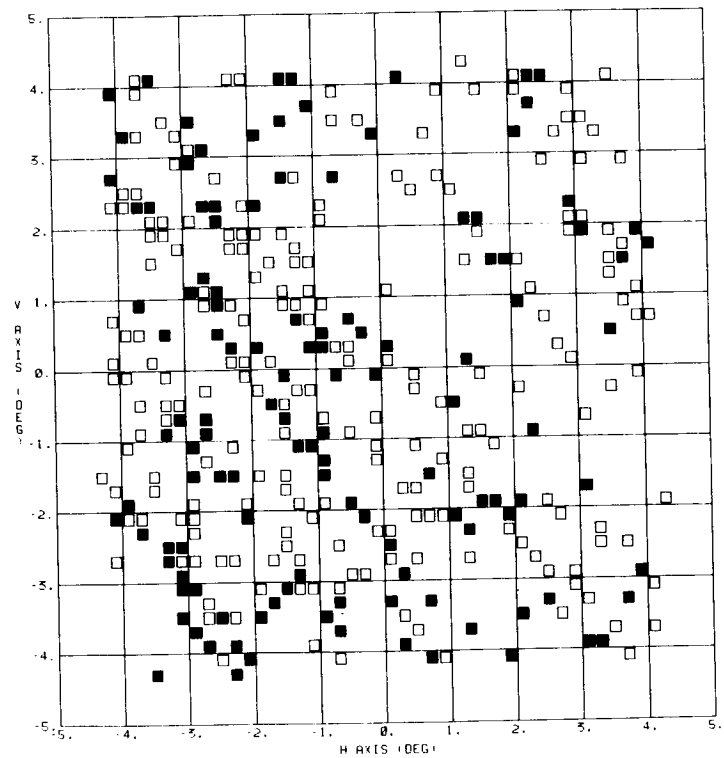

Figure 3. FHST1 Sensitivity Index Plot Using Polynomial Transformation, 1988 Data

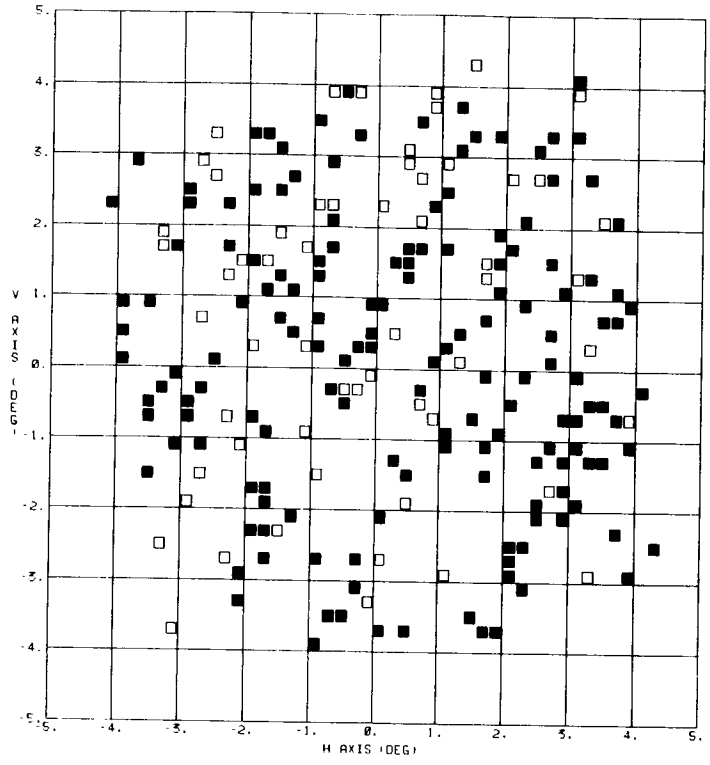

Figure 4. FHST2 Sensitivity Index Plot Using Simple Transformation, 1984 Data

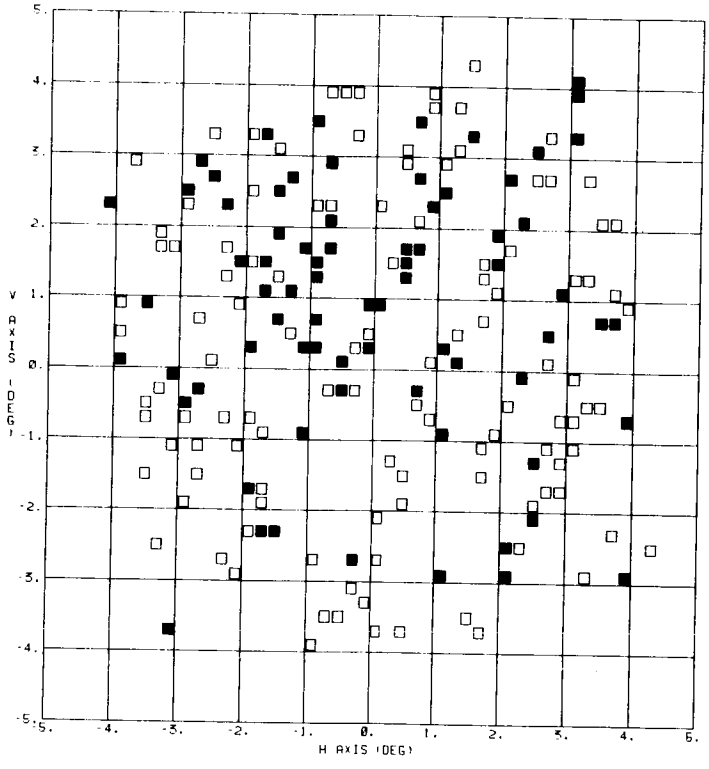

Figure 5. FHST2 Sensitivity Index Plot Using Polynomial Transformation, 1984 Data

Table 2. FHST Sensitivity Values Within 10 percent of Unity

		Original	Simple	Polynomial
FHST1				
October - December	1984	72	72	78
July - September	1985	69	62	73
January - March	1986	57	45	52
July - September	1987	48	64	77
July - September	1988	34	66	90
March - May	1989	29	62	77
FHST2				
October - December	1984	47	45	91
July - September	1985	39	62	85
June - August	1986	27	51	71
June - August	1987	33	65	81

Table 3. FHST1 Sensitivity Values Within 10 Percent of Unity for the H+, V- Quadrant

		Original	Simple	Polynomial
FHST1				
July - September	1985	72	53	81
January - March	1986	18	36	59
July - September	1987	24	41	73
July - September	1988	8	61	91
March - May	1989	22	56	75

manually commanded back to the correct attitude.

Some future missions, most notably the Upper Atmosphere Research Satellite (UARS), will contain an onboard star catalog. Thus, another type of error may occur that did not affect the SMM. Since UARS will be computing onboard attitudes using the star catalog and the intensity-to-magnitude equation, accurate sensing of the correct star magnitude is very important. Thus, misidentification of stars, especially when the FHSTs are observing sparse star fields, will cause an error in the determined attitude.

Thus, it is recommended here that missions with high accuracy requirements should use the polynomial transformation. However, for missions where the requirements are not as stringent, the extra accuracy given by the polynomial fit does not justify the extra effort and memory required.

Affect on Magnitude Response of the Individual Terms

To ascertain why the polynomial transformation is more accurate than the simple transformation, the individual components of the polynomial transformation will be examined. Terms that depend on FOV position and star color are unique to the polynomial

transformation whereas both transformations contain a dependence on the stellar magnitude of the star.

The first term evaluated is the correction for the position coordinates. The analysis in the previous section showed that areas of poor sensitivity were removed by including the position coordinates in the polynomial transformation. However, a quantitative examination of this improvement remains to be performed. Since it contains the most observations, the segment of data from March through May of 1989 will be examined. The polynomial transformation was altered so that only terms accounting for magnitude and star position were included. Table 4 shows that the percentage of good observations improved from 62 percent, using the simple transformation, to 64 percent, using the polynomial transformation with only position correction. However, the complete polynomial transformation improved the results to 77 percent. Thus, the correction due only to position is a small part of the improvement seen using the polynomial transformation.

The polynomial transformation was then adjusted to include only the star color. Table 4 shows that the percentage of good observations improved from 62 percent to 73 percent. Thus, most of the improvement from using the polynomial transformation is due to the star color terms in the equation.

Table 4. FHST1 Sensitivity Values Within 10 Percent of Unity for Star Color or Position Only

			Whole Field
FHST1			
March - May	1989	Star Color only	73
		Position only	64

Fig. 6 shows the dependence of the sensitivity on color. The SMM used a color value known as the blue minus visual magnitude index. This represents the blueness of the star. The more positive the value of the $B - V$, the bluer the star. Fig. 6 shows that the bluer stars, represented by the more positive values of $B - V$, have generally higher values for the sensitivity index. This indicates that the intensity of bluer stars is sensed more accurately by the FHST. Since the simple transformation equation was used to compute the predicted values in the figure, it is expected that more of the bluer star observations will have sensitivity values greater than 1. This is the case as shown in Fig. 6.

The results of the star color analysis have important consequences. The important point to remember is that the NASA standard FHSTs sense the intensity of bluer stars more accurately. The results presented here confirm the analysis done previously by Lorenz[6] and Neste[7]. Lorenz (Ref. 6) first discovered the effect of star color on FHST observations in his analysis of the intensity variations seen by the Landsat-4 FHST observations. Neste (Ref. 7) adapted that work for use on the UARS mission and even presented a quantitative result. The resulting equation computed a correction to the star magnitude based on the star color.

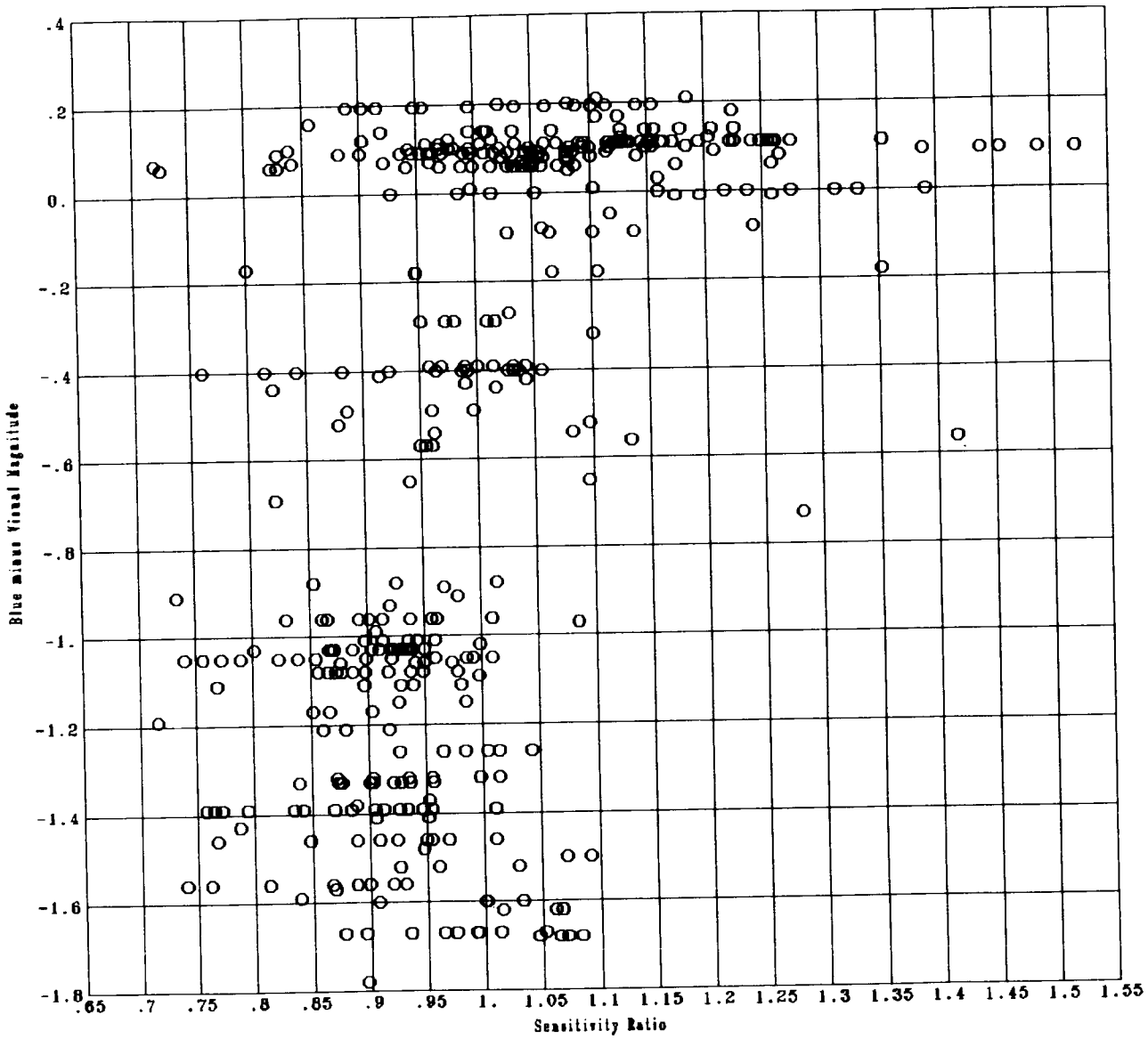

Figure 6. Dependence of Sensitivity Index on Color

5. FHST AGING

As with any electro-mechanical device exposed to the space environment, the SMM FHSTs suffered performance degradation in response to problems that may be associated with aging. Aging causes changes in the sensitivity of the sensor that require calibration to correct the observed intensity. However, if the simple transformation equation is used without recalibration on each segment of data, the resulting measurement degradation of the later segments can provide clues about the aging processes of star cameras in general.

For the evaluation of the aging process, each FHST was calibrated using the October through December 1984 data. With these calibration coefficients, the simple transformation was used to compute the predicted intensities for all the remaining data segments. As expected, the sensitivity response for both FHSTs degraded significantly. As shown by the systematic darkening of Fig. 7 through Fig. 9, the FHST1 response was significantly degraded over the lifetime of the SMM. This is the real degradation of the sensor. In practice, the SMM FHST performance was maintained by calibrating the response every few months.

As the figures illustrate, the SMM FHST1 degradation was very significant. This FHST appeared to age faster in the lower-right quadrant (the +H,-V). Table 2 shows this aging for each segment, and these statistics indicate that the FHST became completely unusable after several years. Table 3 shows that the lower-right quadrant aged faster and became unusable in about 1 year.

The results for FHST2 differ from those of FHST1. Table 2 shows that the FHST2 sensitivity response degraded only slightly over the years. Fig. 10 through Fig. 12 confirm this pattern. While the sensitivity response of FHST2 did degrade, it was not as profound as that of FHST1. This behavior can be partially explained by the alignment of the two FHSTs. The angle between the sensor boresight and the spacecraft to Sun direction was smaller for FHST1 than for FHST2 by approximately 73 deg. Thus, it is possible that more stray sunlight entered FHST1 causing it to age faster.

The causes of aging in star cameras are factors such as temperature variations, space radiation, bright light impingement, space debris collisions, and any other effects native to the space environment. Thus, it may be concluded from this analysis that NASA SSTs age at different rates and, in addition, separate areas of the same FHST may age differently.

CONCLUSIONS

This paper has presented a study of the sensitivity response of the fixed-head star trackers flown on the Solar Maximum Mission. Three studies were performed, and the results may be used by future missions to aid in the performance analysis of any type of star camera. The first study examined two separate intensity-to-magnitude transformation equations and the results indicated that the polynomial transformation provided better results than the simple transformation. On the basis of these results, the polynomial transformation was recommended for use on missions with stringent attitude requirements so that errors due to misidentification of stars may be avoided. The second study was an examination of the individual affects of star color and position on sensitivity. This study showed that star color was the more important effect, and correction for it, either by using

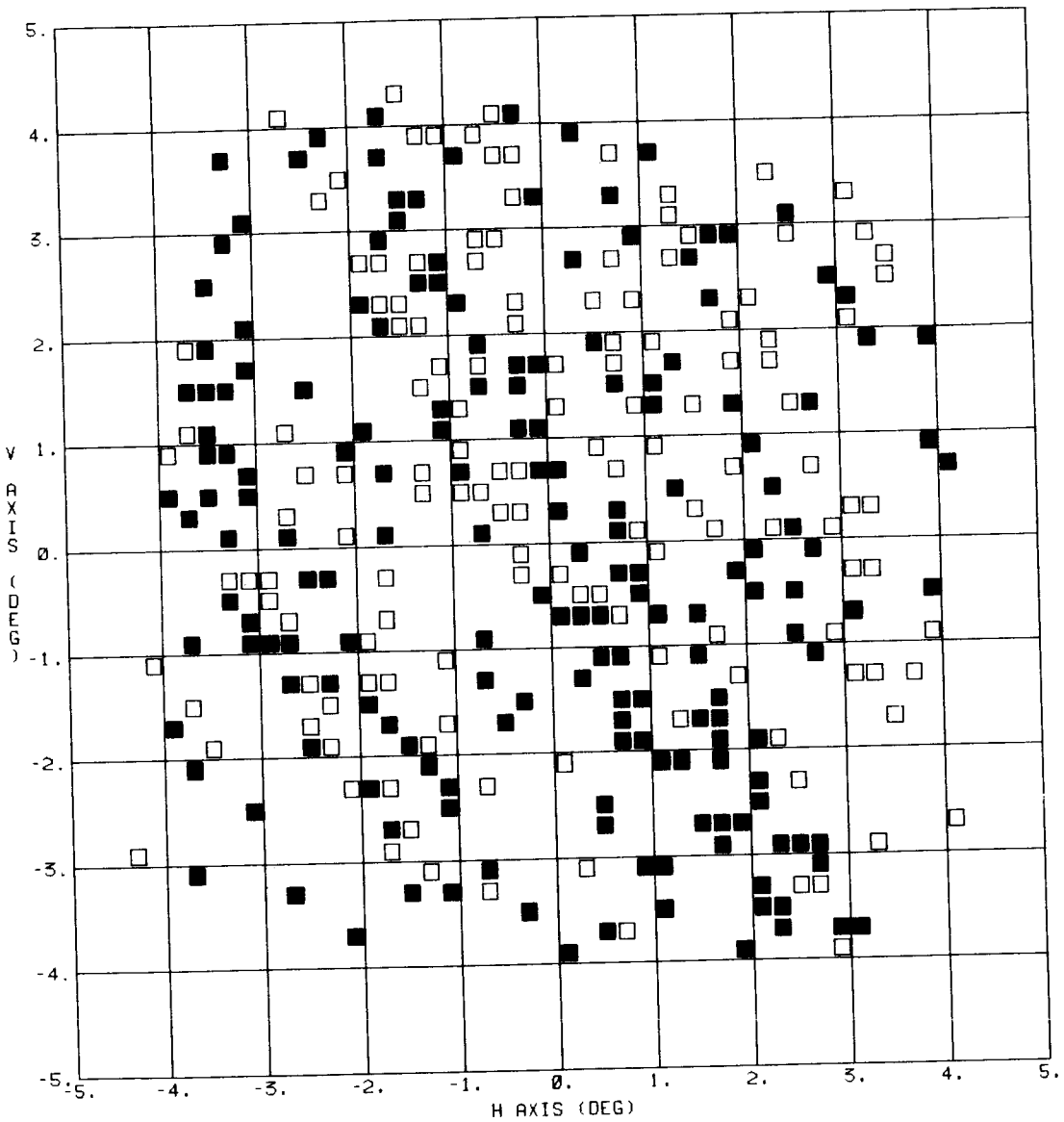

Figure 7. FHST1 Sensitivity Index Plot, Original Transformation Coefficients, 1984

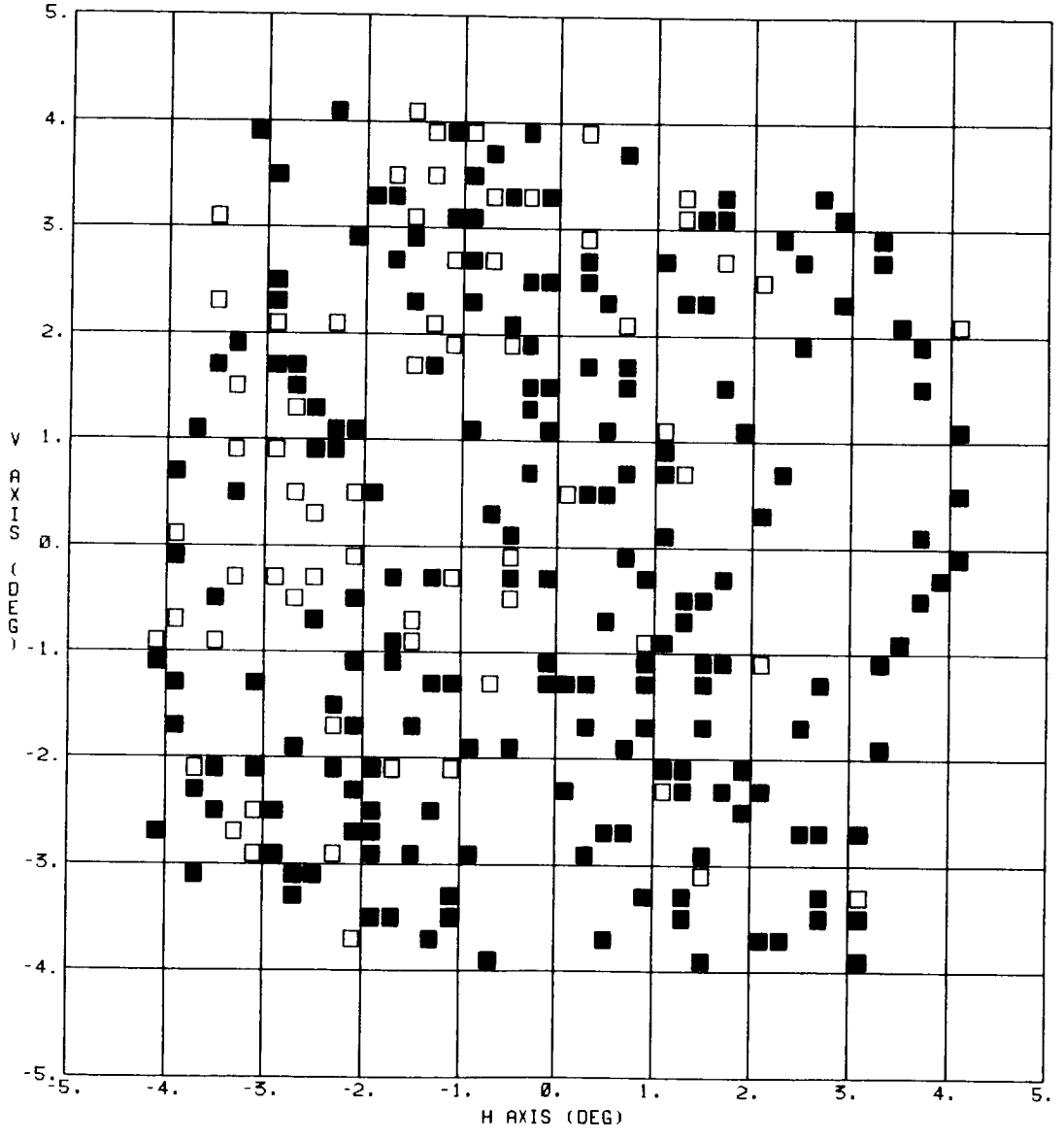

Figure 8. FHST1 Sensitivity Index Plot, Original Transformation Coefficients, 1987

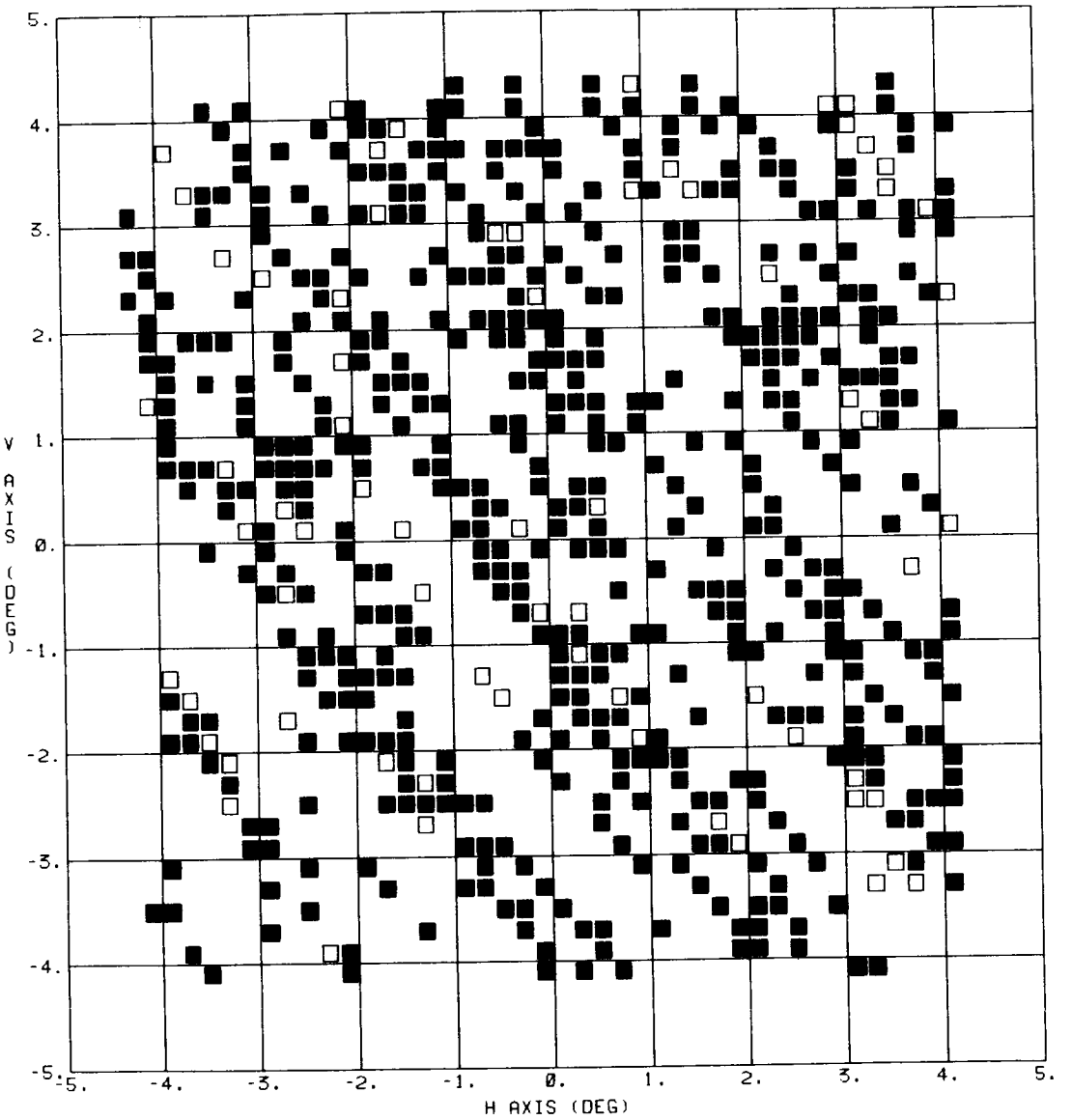

Figure 9. FHST1 Sensitivity Index Plot, Original Transformation Coefficients, 1989

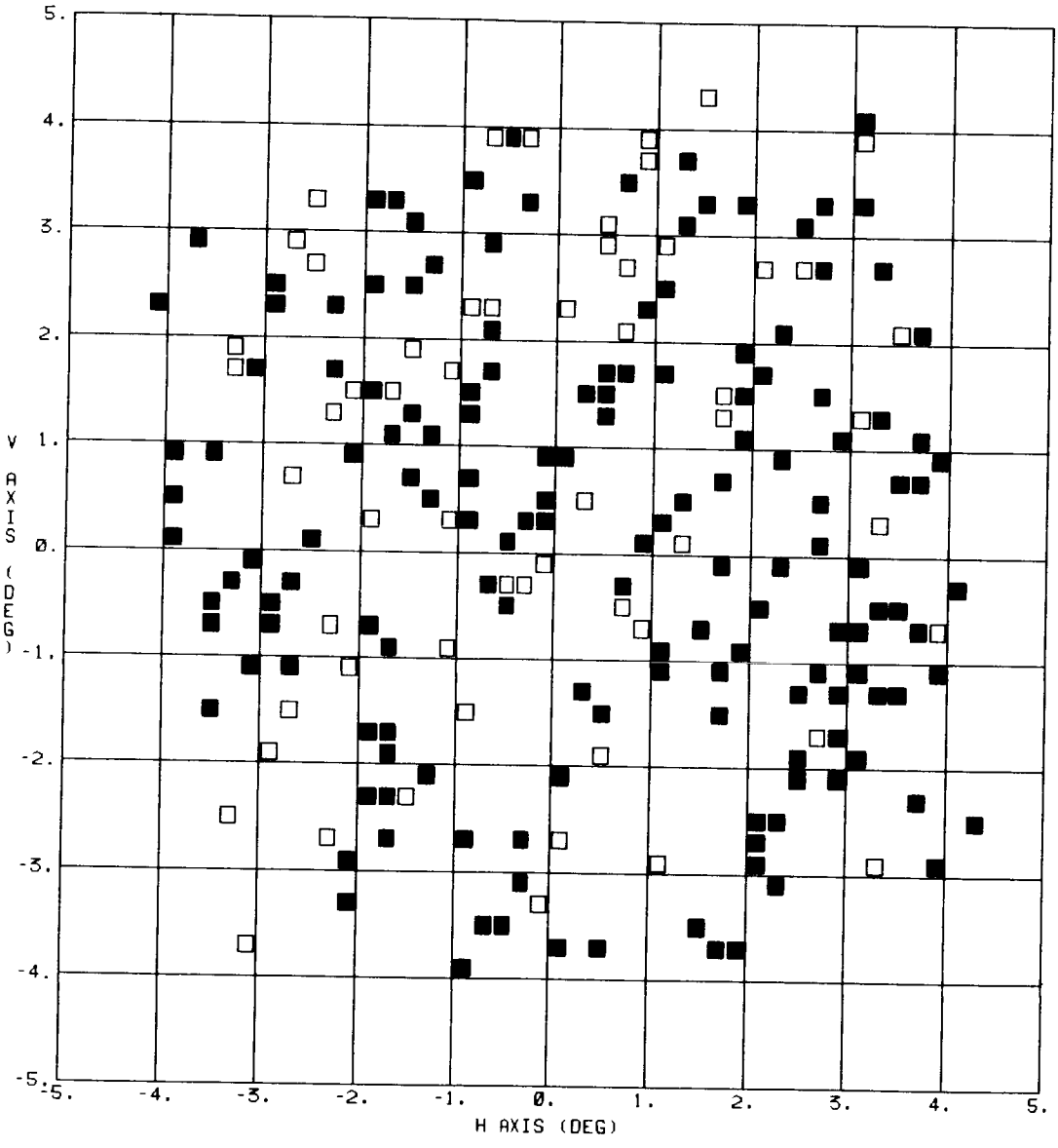

Figure 10. FHST2 Sensitivity Index Plot, Original Transformation Coefficients, 1984

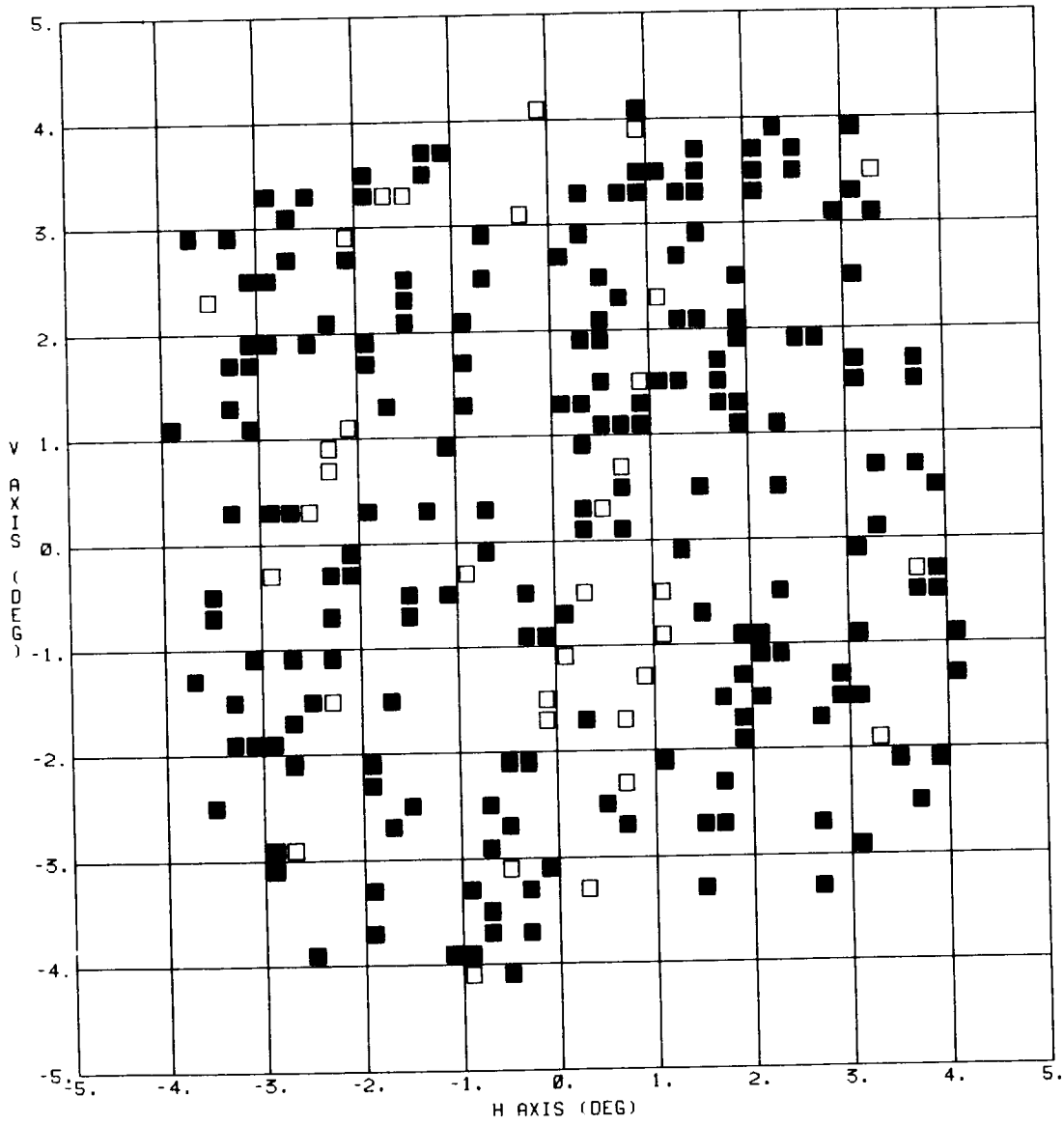

Figure 11. FHST2 Sensitivity Index Plot, Original Transformation Coefficients, 1985

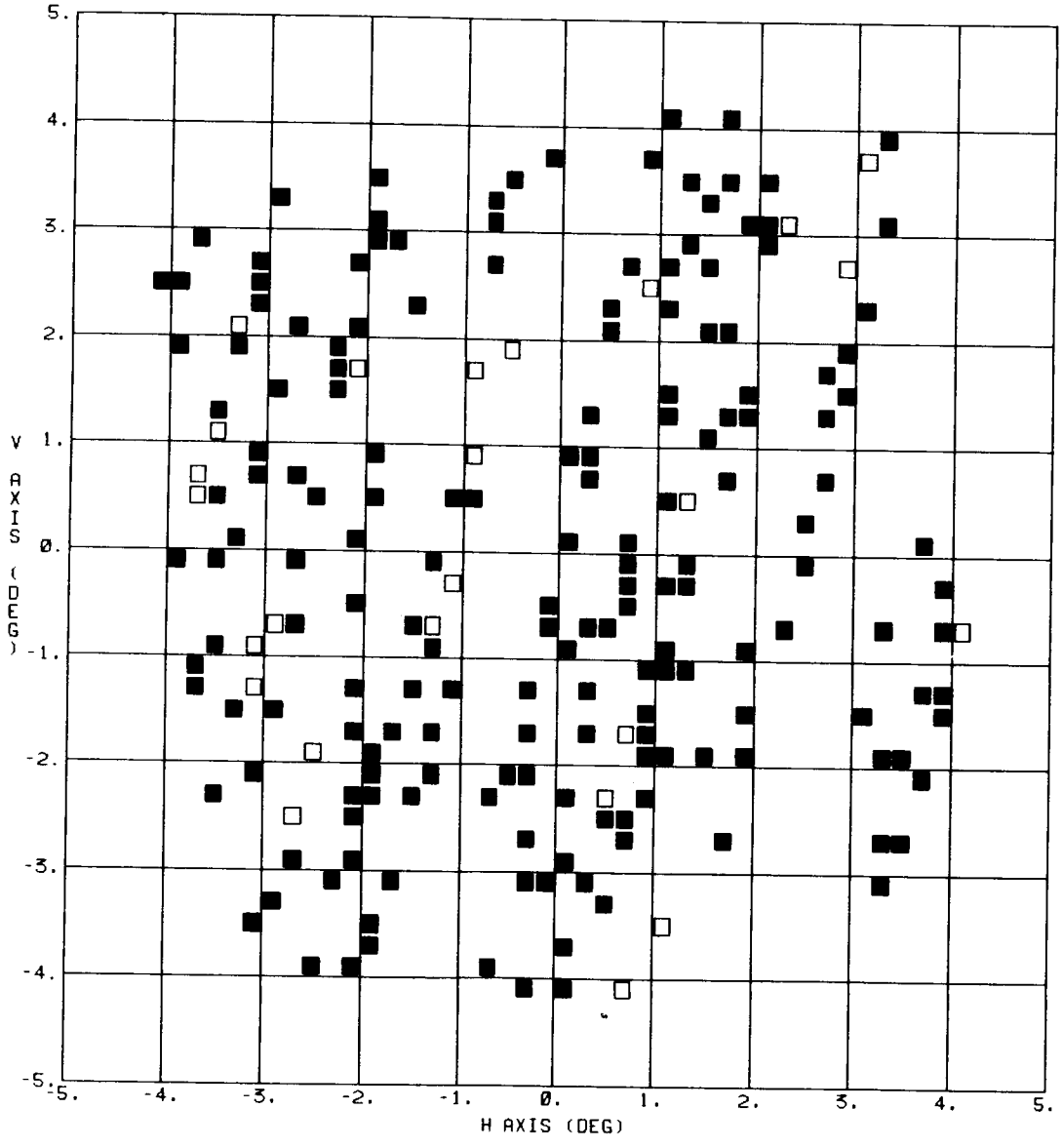

Figure 12. FHST2 Sensitivity Index Plot, Original Transformation Coefficients, 1986

showed that star color was the more important effect, and correction for it, either by using the polynomial transformation equation or a separate equation correcting the final magnitude, is important. The third study examined the aging of star trackers and concluded that aging due to the effects of the space environment was apparent, and that the sensors age at different rates with different characteristics. Therefore, the aging process of each sensor should be studied closely throughout the mission.

ACKNOWLEDGEMENTS

The authors wish to thank the following people for their criticisms and suggestions regarding the material in this paper: Dave Lorenz (GSFC), Mark Slater (CSC), Karen McDaniel (CSC), Milt Phenneger (CSC), Robert Shendock (OAO), and Robert Feiertag (CSC).

REFERENCES

[1] Pitone, D., *Solar Maximum Mission End-of-Mission Document*, Computer Sciences Corporation, CSC/TM-90/6058, March 1990.

[2] *User's Guide for Standard Star Tracker*, Ball Aerospace Systems Division, TM79-04.

[3] Wertz, J.R., ed., *Spacecraft Attitude Determination and Control*, D. Reidel, Dordrecht, the Netherlands, 1978.

[4] McLaughlin, S. and Slater, M., *Skymap System User's Guide, Revision 1*, Computer Sciences Corporation, CSC/SD-89/6076, September 1989.

[5] McCutcheon, R., *SMM Fixed Head Star Tracker Field of View Sensitivity Analysis*, Computer Sciences Corporation, CSC/TM-81/6052, March 1981.

[6] Lorenz, D., *Landsat Attitude Sensor Performance - Evaluation III*, Computer Sciences Corporation, PCA/IM-85/046, September 1985.

[7] Neste, S., *Color Index Computation for the NASA Standard Fixed Head Star Trackers on UARS*, General Electric, PIR NO: U-1k21-UARS-855, June 1987.